CO_2 Human Emissions

Fingerprints of fossil CO_2 sources

A.T.J. de Laat
R.J. van der A

Co-ordinated by ECMWF

D3.4 Fingerprints of fossil CO_2 sources

Dissemination Level:	Public
Author(s):	Jos de Laat, Ronald van der A (KNMI)
Date:	20/12/2019
Version:	1.0
Contractual Delivery Date:	31/12/2019
Work Package/ Task:	WP3/T3.3
Document Owner:	KNMI
Contributors:	KNMI
Status:	Final

CHE: CO_2 Human Emissions Project

Coordination and Support Action (CSA)
H2020-EO-3-2017 Preparation for a European capacity to monitor CO2 anthropogenic emissions

Project Coordinator: Dr Gianpaolo Balsamo (ECMWF)
Project Start Date: 01/10/2017
Project Duration: 39 months

Published by the CHE Consortium

Contact:
ECMWF, Shinfield Park, Reading, RG2 9AX,
gianpaolo.balsamo@ecmwf.int

The CHE project has received funding from the European Union's Horizon 2020 research and innovation programme under grant agreement No 776186.

Table of Contents

Figures

Tables

1 Executive Summary

Anthropogenic CO_2 and NO_2 emissions from combustion processes have usually the same sources but with different emission ratios. By applying the known emission ratios of CO_2 and NO_2 from established emission databases to the satellite-derived NO_2 emissions we derive CO_2 emissions based on satellite observations of NO_2. We have used the inverse algorithm DECSO to the high resolution NO_2 observations of TROPOMI. We have analyzed DECSO-TROPOMI NO_2 emissions for the Iberian Peninsula and an area over South America. We have derived CO_2 emissions based on multiplying the DECSO-TROPOMI NO_2 emissions with CO_2 over NO_2 emission ratios derived from a TNO emissions database.
We find that the spatial distribution of DECSO-TROPOMI based CO_2 emissions of the Iberian Peninsula and the South America region overall appears realistic, especially if they are corrected for NO_2 soil emissions.
Some uncertainties are added by the fact that spatial patterns of emissions ratios revealing strong inter-country differences. It was also shown that the ratios can vary a lot over time, and therefore the year of the ratios and NO_2 emissions should be the same.

2 Introduction

2.1 Background

Climate change is a dominant global environmental issue, for which international treaties have been signed in order to try to reduce carbon dioxide (CO_2) emissions worldwide and limit global temperature rise.

Monitoring CO_2 emissions – and thus reporting them – is complicated due to the wide variety of processes causing CO_2 emissions. Anthropogenic combustion emissions cause CO_2 to rise, but are difficult to distinguish amidst natural biogeochemical sources. Furthermore, this wide variety of CO_2 emission sources limits the use of local CO_2 observations. A proper monitoring system would require at least a very dense network of observations. But even then, because of the long atmospheric life time of CO_2, monitoring very localized sources remains complicated, if not impossible.

Satellite observations may open new possibilities of global monitoring of CO_2. During the last decade, several satellites have been launched that can measure CO_2, some of them even specifically tasked with mapping CO_2 worldwide. Additional dedicated and innovative satellite missions are in preparation. Nevertheless, translating these satellite measurements back to localized CO_2 emissions remains difficult for similar reasons: the wide variety of CO_2 sources worldwide, and its long atmospheric lifetime.

Therefore, alternative (indirect) methods for derive CO_2 emissions from satellite observations are starting to be considered. One particularly interesting possibility is to use satellite measurements of another trace gas (Nitrogen Dioxide, or NO_2), determine the corresponding NO_2 emissions, and the convert these NO_2 emissions into CO_2 emissions using predefined emission ratios. Because NO_2 in urbanized regions is to a large extent emitted by anthropogenic combustion processes, such a method might deliver NO_2-based anthropogenic CO_2 combustion emissions.

2.2 Scope of this deliverable

2.2.1 Objectives of this deliverables

Task 3.3 specifies the following activities: [1] Identification of space infrastructures providing NO_2 observations, the associated characteristics and performances (spatial and spectral resolution, temporal sampling, accuracy) focusing on the European space infrastructure such as Copernicus (Sentinel-4 and Sentinel-5). [2] use CO_2/NO_2 emission ratios (from Task 3.2) to associate specific CO_2 emissions with the derived NO_2 emissions and estimate uncertainties for deriving combustion CO_2 emissions .

2.2.2 Work performed in this deliverable

The recently launched TROPOMI instrument is providing measurements of tropospheric NO_2 of unprecedented quality, which allow for more accurate determination of tropospheric NO_2 columns at higher spatial and temporal scales. Actually, TROPOMI has proven capable of providing daily fields of tropospheric NO_2 with a spatial resolution down to 3.5×5.5 km. TROPOMI tropospheric NO_2 columns thus provide an excellent starting point for exploring such new methods. The NO_2 columns are used in inverse modelling to derive regional emissions of NO_2 on a high resolution grid of 0.125 x 0.125 degree.
In this report we present results of a first attempt to derive CO_2 emissions derived from satellite-based NO_2 emissions using TROPOMI tropospheric NO_2 column measurements and CO_2/NO_2 emission ratios.

2.2.3 Deviations and counter measures

There were no deviations.

3 Method and data

3.1 Emission data

For the CO_2 over NO_2 emission ratios over the Iberian Peninsula we rely on detailed TNO emission databases for the years 2010 and 2015, provided by TNO [H. Denier van der Gon]. This data consists of gridded sector-based emissions of air pollution and greenhouse gas emissions over Europe. These emissions are converted into one set of European NO_2 emissions and one set of European CO_2 emissions. However, in the future the method can be improved by using more information from the sector-based information embedded in the TNO database.

For South America we use CO_2 and NO_2 emissions from the EDGAR-HTAP-v2 database (http://edgar.jrc.ec.europa.eu/htap_v2/). More details about EDGAR-HTAP-v2, see Janssens-Maenhout et al. [2015].

3.2 TROPOMI and future satellite observing capacity

The TROPOMI instrument (or Sentinel-5 Precursor mission) is a UV-VIS spectrometer build on the heritage of previous missions like OMI, GOME-2, SCIAMACHY, and GOME. TROPOMI orbits the earth in a low earth orbit, providing approximately 14 orbits per day with a swath width of approximately 2700 km, enough to almost provide global coverage in one day. Best pixel sizes (sub-satellite point) were 3.5×7 km, during the summer of 2019 further improved to 3.5×5.5 km. Right from the beginning, TROPOMI has been providing measurements of unprecedented quality, including measurements of tropospheric NO_2

columns. More details about the TROPOMI instrument can be found in Veefkind et al. [2015].

For the coming decade, there are several new satellite missions planned with NO_2 observing capacity (Table 1). For TROPOMI (Sentinel 5P) there will be the follow up mission sentinel 5. There will also be other low orbit missions from the USA and China, although not with the high spatial resolution of TROPOMI.

In addition, for North America, Europa, and east Asia, there will be geostationary hyperspectral missions providing hourly daytime temporal resolution rather than daily resolution. The spatial resolution of these geostationary missions is approximately similar to the TROPOMI pre-launch spatial resolution (7×7 km), which later was upgraded to the current TROPOMI spatial resolution of 3.5×5.5 km. Although hyperspectral geostationary satellite observations is a new branch of the earth observation tree and experience with data quality is limited, they provide potentially exciting new possibilities.

At the other end of the spectrum are kilometer-scale low orbit missions focusing on CO_2 emissions but which have a NO_2 channel to identify anthropogenic sources. These missions do not provide global daily coverage but provide excellent resolution to resolve small scale emission sources.

3.3 DECSO

TROPOMI tropospheric NO_2 column measurements can be calculated back to localized emissions using the Daily Emission estimation Constrained by Satellite Observations inversion algorithm [DECSO; Mijling and van der A, 2012]. This algorithm, developed at KNMI, has been applied to tropospheric NO_2 column observations of OMI and GOME-2, and used for a wide variety of applications. Aspects of the validation of the latest version 5.0/5.1 applied to satellite measurements of NO_2 for inversions of NO_2 emissions are described in Ding et al. [2017a, 2017b, 2018].

Because satellites cannot directly measure emissions, simulation is usually needed to calculate a concentration field from a certain emission inventory. The difference between observed and modeled concentrations contains information for adjusting the underlying emissions. This is especially relevant when transport from the source becomes important and non-local sensitivities of concentration to emission must be calculated. This is typically the case for shorter time scales or for satellite measurements with (finer) spatial resolutions where trace gas plumes due to transport are resolved. Because of the transport away from the source, however, this inversion problem is computationally complex, and a single forward model run does not provide information on the (non-local) dependence of concentration on emissions, in particular for sources not present in a priori emission databases.

The DECSO algorithm combines the sensitivity of NO_2 column concentrations on local and nonlocal NO_2 emissions using a simplified isobaric surface 2-D trajectory analysis. The DECSO algorithm allows for calculating local and non-local sensitivities of concentration to emission based on a single forward chemistry-transport model run from the CHIMERE model, without using adjoint model code or perturbation techniques. Hence, there is no need to calculate explicitly the sensitivities nor the evolution of the emission covariance. Sensitivities are available everywhere regardless on whether or not there are emissions in CHIMERE. As a consequence, DECSO is able to detect new emission sources which are not present in the emission database of the CHIMERE model simulation. In fact, there are no a-priori emissions needed in DECSO. Note that both the 2-D trajectory analysis and the

CHIMERE model use wind data from weather analyses of the European Center for Medium range Weather Forecasts (ECMWF).

Important advantages of the DECSO algorithm are further that it can be applied to mesoscale emission inventories, and works at least for short-lived chemical species. It is fast enough to enable daily assimilation of satellite observations. Finally, it converges sufficiently fast toward the new emission levels to enable short-term emission trend analysis.

3.4 Dataset details

For this report, we use the following data:

- TNO annual emission databases for 2010 and 2015 on a 0.1°×0.1° resolution
- EDGAR-HTAP v2 emission database for 2010 on a 0.1°×0.1° resolution
- TROPOMI tropospheric NO2 column measurements for July 2018 to June 2019
- DECSO-TROPOMI annual NO2 emissions on a 0.125°×0.125° resolution (daily to annual). The period of this data sets covers July 2018 to June 2019.

Both emission databases used here are resampled to the 0.125°×0.125° resolution of DECSO emissions.

4 Results: Iberian Peninsula

4.1 NO_2 emissions

Figure 1a shows the DECSO-TROPOMI NO_2 emissions for 2018/2019 on a 1/8 degree resolution (0.125°) for the Iberian Peninsula, while Figure 1b shows the corresponding TNO 2010 anthropogenic NO_2 emissions. The DECSO NO_2 emissions are provided in grams N/month and converted to grams NO_2 using the molecular mass ratios of NO_2 and N (46.0055/14.0067).

The spatial variations in both plots appear similar with clearly discernible populated (industrial) regions and shipping routes (note the logarithmic color scale used for both plots). However, it is also evident that outside the industrialized land regions, the DECSO-TROPOMI emissions are larger than the TNO emissions. This is related to biogenic (soil) NO_2 emission which are especially large during summer.

Figure 2 clearly reveals both the agreement and discrepancy between NO_2 emissions from TNO and DECSO-TROPOMI. For NO_2 emissions larger than approximately 5 10^8 g NO_2/grid/year both TNO 2010 and DECSO results agree fairly well. However, DECSO-TROPOMI emissions clearly level off around 1 10^8 g NO_2/grid/year, where TNO 2010 anthropogenic NO_2 emissions do not show such levelling off. The correlation between both emission datasets is 0.60 for all data, and 0.58 and 0.18 for TNO emissions larger and smaller than 1 10^8 g NO_2/grid/year. This shows that indeed for smaller TNO emission values there is hardly any correlation with the DECSO emissions as a results of the biogenic emissions included in the DECSO emissions.

This finding will later on become relevant for the conversion of DECSO-TROPOMI NO_2 emissions to CO_2 emissions using the TNO 2010 CO_2 over NO_2 ratio emission ratio: certain biogenic NO_2 emissions derived with DECSO cannot be attributed to CO_2 and need to be accounted for. This will be discussed in more detail later on.

4.2 CO_2 emissions using the CO_2 over NO_2 emission ratio

Figure 3a shows the DECSO-TROPOMI – based CO_2 emissions using the TNO CO_2 over NO_2 ratio, while Figure 3b displays the corresponding TNO 2010 CO_2 emissions. As with the NO_2 emissions comparison in Figure 1, there are clear similarities and differences.

The large urbanized industrial areas and shipping routes clearly stand out. Over land, DECSO-TROPOMI – based CO_2 emissions outside of industrialized areas are clearly larger than the TNO 2010 anthropogenic CO_2 emissions due to biogenic NO_2 emission (which will be discussed in more detail in section 4.3.1). As discussed, this is related to biogenic NO_2 emissions that by application of the ratio-method are converted into CO_2 emissions.

Also, DECSO-TROPOMI – based CO_2 emissions over the oceans reveal emissions throughout the oceans that in the TNO 2010 anthropogenic CO_2 emissions are much smaller (< 10%). It is important to note that the TNO database indicates that there are shipping emissions outside the shipping lanes around the Iberian peninsula, but these are so small that they do not show up in Figure 3b.

Figure 4 shows the probability distribution of DECSO-TROPOMI – based CO_2 emissions and TNO 2010 anthropogenic CO_2 emissions. There are two separated distributions related to urbanized regions and shipping lanes on the one hand, and background/rural regions on the other hand. Both distributions show a levelling off of DECSO-TROPOMI based emissions not present in the TNO data, which is related to the previously discussed biogenic emissions in DECSO data that is not present in the TNO data (*cf.* Figures 1 and 2). Furthermore, the DECSO- based CO_2 emissions also appear to be biased high compared to the TNO 2010 CO_2 emissions.

Figure 5a and 5b shows the spatial variations in CO_2 emissions for both DECSO and TNO (2010), respectively, while disregarding CO_2 emissions larger than 5 10^6 kg CO_2/grid/year. The spatial structures are much more similar, revealing industrialized urbanized regions, corridors between industrialized urbanized regions, and the shipping lanes. The existence of these corridors is attributed to both roads (highways) connecting the major urbanized industrial regions and smaller towns and cities that have developed along these connections.

Figure 6a and 6b show the relative differences (6a) and absolute differences (6b) between CO_2 emissions for both DECSO and TNO (2010) as presented in Figures 5a and 5b. Clearly there are significant emission differences in various areas of several tens of percents, pointing to potentially areas for further research.

4.3 Biases and other issues

4.3.1 Biogenic NO_2 soil emissions

From the previous sections it is clear that NO_2 originating from biogenic emissions observed by TROPOMI needs to be accounted for, as they are not present in the TNO anthropogenic NO_2 emission database.

Because biogenic NO_2 emissions are usually related to microbial soil activity, to some extent those soil emissions will be ”anti-correlated” with anthropogenic NO_2 emissions. In industrialized regions, soils are often covered, reducing biogenic NO_2 emissions. Reality is more complex, as also vegetation plays a role, and anthropogenic NO_2 emissions can be very localized and thus occur in regions with significant biogenic emissions (for example: a highway through a remote area).

One possible approach would be to select or filter the emission data based on both CO_2 emissions values and NO_2 emission values. For example, Figure 2 suggests that biogenic NO_2 emissions lead to baseline NO_2 emissions of 10^8 g/grid/year. That threshold could be applied the TNO NO_2 emissions by only considering grids for which TNO NO_2 emissions exceed 10^8 g/grid/year. In addition, Figure 4 suggests that DECSO-based CO_2 emissions level off at 5 10^6 kg/grid/year, which could be used to also disregard grids with TNO CO_2 emissions smaller than 5 10^6 kg/grid/year while also subtracting a CO_2 emission value of 5 10^6 kg/grid/year. We thus assume here in effect that only DECSO-TROPOMI emissions above these thresholds reflect dominantly anthropogenic emissions.

Figure 7 shows the resulting probability distribution of DECSO-TROPOMI based CO_2 emissions and TNO 2010 CO_2 emissions. Clearly the bias associated with biogenic NO_2 emissions has vanished, and the distribution suggests a better spatial correspondence between TNO 2010 CO_2 emissions and DECSO-TROPOMI based CO_2 emissions. Correlations are 0.87 (logarithmic) and 0.79 (linear).

This is only one possible approach for how to account for biogenic NO_2 emissions. Additional research will explore other approaches and test how sensitive results are for different approaches.

4.3.2 Spatial distribution of TNO CO_2 over NO_2 emission ratios

Figure 7 does still result in larger DECSO-TROPOMI based CO_2 emissions compared to TNO 2010 CO_2 emissions. Although in the log-log scale it does appear to be relatively small, in absolute sense these differences are still significant and relevant (see also table 2).

To investigate whether this is a real difference or the results of the applied method, we further explored the TNO emission database. Figure 8 shows the European wide distribution of TNO 2010 CO_2 over NO_2 emission ratios.

There is much that could be discussed here and worth of detailed research, but for now we suffice to conclude the following: the patterns reveal clearly differences related to different physical processes resulting in different ratios. For example, in France, ratios are larger for urbanized regions compared to the countryside. Similarly, inland shipping lanes, as well as roads, show different ratios compared to surrounding regions.

Figure 8 also reveals that there are significant inter-country differences. Ratios jump from country to country and sometimes even from region to region. Since the TNO emissions are (also) based on country-based reports and databases, this strongly suggests that there exist considerably differences in emission registration methods and/or emission calculation methods – either for CO_2 or NO_2, or both.

4.3.3 Time differences in the spatial distribution of emissions

To further explore the inter-country dependency of CO_2 over NO_2 emission ratios we also present results for the 2015-2010 relative differences in TNO CO_2 emissions (Figure 9a), TNO NO_2 emission (Figure 9b), and the relative differences between 2015 and 2010 emission ratios (Figure 9c). Note that the latter effectively reflects the ratio of 2015/2010 TNO CO_2 emissions over the 2015/2010 TNO NO_2.

Although both CO_2 over NO_2 emissions in Europe mostly decrease between 2010 to 2015, we see that similar to the spatial patterns of the TNO CO_2 over NO_2 emission ratios in Figure 8, there exist large inter-country differences between 2010 and 2015 emissions. This provides additional support to the previous suggestion that considerably differences exists in emission registration methods and/or emission calculation methods – either for CO_2 or NO_2, or both.

How this translates in to uncertainties in DECSO-TROPOMI based CO_2 emissions is unclear. We see that in absolute sense NO_2 emissions over Europe have decreased between 2010 and 2015, over large areas with 25% or more. However, based on application of the emission ratios for 2010 and 2015 and applying them to one year of DECSO-TROPOMI NO_2 data (July 2018-June 2019), we find that CO_2 emissions actually would have increased. The decrease in NO_2 emissions is significantly larger than the decrease in CO_2 emissions, which might points to filtering techniques of NO2 in the industry, power plants, and the transport sector. The resulting effect is that emission ratios change from year to year. However, the comparison reveals the TNO data captures year to year changes in emissions of both gases, and that those change can be independent of each other. The comparison also proves that it will be crucial to apply emission ratios to the years they represent.

5 Results: South America

We also derived DECSO-TROPOMI based anthropogenic CO_2 emissions for a part of South America: the southern end of Brazil including the cities Rio de Janeiro and Sao Paolo, Uruguay, part of Paraguay including its capital Asuncion, and a small part of Argentina near its capital Buenos Aires.

For the CO_2 over NO_2 emission ratio we rely on the EDGAR-HTAP v2 database for the year 2010. Figure 10a shows the EDGAR-HTAP-v2 anthropogenic CO_2 emissions for the region. As for Europe (Figure 3b), these emissions are dominated by the large industrialized urbanizations. With the logarithmic color scale, also corridors connecting these urbanizations can be seen, as well as shipping routes.

Figure 10b shows the corresponding DECSO-TROPOMI based CO_2 emissions. Similar to what was observed over the Iberian peninsula, these emissions show both the large industrialized urbanizations but also larger background emissions due to biogenic NO_2 emissions. Applying a cutoff CO_2 emission threshold of 5×10^6 kg/grid/year and subtracting this CO_2 emission threshold from the DECSO-TROPOMI CO_2 emissions reveals spatial variations for EDGAR-HTAP-v2 (Figure 11a) and DECSO-TROPOMI based CO_2 emissions (Figure 11b) that at first glance appear rather similar.

Figure 12 shows the probability distribution of both EDGAR-HTAP-v2 (Figure 11a) and DECSO based CO_2 emissions (Figure 11b). These distributions are very similar, indicating that DECSO based CO_2 emissions spatial distribution when disregarding the non-anthropogenic background NO_2 emissions are comparable, but also that absolute emission amounts of DECSO-TROPOMI based CO_2 emissions agree with EDGAR-HTAP-v2 anthropogenic CO_2 emission estimates. It also indicates that it is important to carefully investigate how to handle/correct for non-anthropogenic (fire, soil) emissions of NO_2, for which more research is needed.

6 Area totals and uncertainties

Based on the first results of the ratio method presented here, we can also estimate budgets of total CO_2 and NO_2 emissions for the Iberian region, and compare them. Table 3 shows Iberian total CO_2 and NO_2 emissions budgets for the region considered in this report for both 2010 and 2015, and with and without applying certain filters.

Results show that without correcting for the background biogenic soil NO_2 emissions, TROPOMI DECSO based CO_2 emissions are 70-92% larger than corresponding TNO CO_2 emissions. Using a simple emission threshold technique (either using only NO_2 or both NO_2 and CO_2) reduces this bias to 9-15%, although if properly done the NO_2 data filter should be applied to TNO NO_2 emission as well, in which case the bias remains larger between 30-47%. Note that spatial correlations between both sets of CO_2 emissions is approximately 0.79.

The comparison between the NO_2 emissions themselves shows that the accounting for background biogenic soil NO_2 emissions, the industrial NO_2 emissions are comparable (bias 1-5%). Based on these results, the background biogenic soil NO_2 emissions are approximately 45%^of total NO_2 emissions over Iberia.

Clearly the background biogenic soil NO_2 emissions should be accounted for. To what extent the remaining bias in TROPOMI DECSO based CO_2 emissions reflects a true bias or can be attributed to uncertainties and assumptions made should be subject of future research.

Table 1. Future space infrastructure providing tropospheric NO_2 observations. Note that the launch date and mission duration details of CO2M are uncertain as it had just been approved at the moment of writing. Sources: ESA, EUMETSAT, NOAA, NASA, KMA, CNSA, WMO (OSCAR), DEOS

	planned mission duration	spatial resolution	temporal resolution	Accuracy	wavelength range/ spectral resolution	remarks
Sentinel 5P	2017-2024	3.5×5.5 km (sub-satellite)	daily global coverage	1×10^{15}	270-495 nm/0.55nm	polar sun-synchronous ESA
OMPS	2011-2019 (SNPP) 2017-2024 (NOAA20) 2022-2029 (JPSS-2) 2026-2033 (JPSS-3) 2031-2038 (JPSS-4)	50 km (nadir/SNNP/NOAA) 17 km (nadir /JPSS)	daily global coverage	1×10^{15}	300–380 nm/1 nm	polar sun-synchronous NOAA/NASA
EMI	2018-2026 GF-5	48×13 km (sub-satellite)	daily global coverage	1×10^{15}	240-403 nm/0.3 nm 401-790 nm/0.5 nm	polar sun-synchronous CNSA
GEMS	2020-2031	7×8 km (sub-satellite)	1 hour	1×10^{15}	300-500 nm/0.6 nm	geostationary east Asia - centered Korea KMA
TEMPO	2020-2027	8.3×4.7 km (sub-satellite)	1 hour	1×10^{15}	290-490 nm/0.6 nm	geostationary North America - centered USA NASA
Sentinel 5	2022-2029 EPS-SG-A1 2029-2036 EPS-SG-A1 2036-2043 EPS-SG-A3	7.5 km (nadir)	daily global coverage	1.5×10^{15} or 30-50%	300-400/0.5 nm	polar sun-synchronous EUMETSAT
Sentinel 4	2023-2031 (MTG-S1) 2031-2039 (MTG-S2)	8×8 km (sub-satellite)	1 hour	15-25%	305-500 nm/0.5 nm	geostationary Europe EUMETSAT
CO2M	2026-2030 (ESA)	1 km (nadir)	200 km swath	1.5×10^{15}	405-490 nm/0.6 nm	polar sun-synchronous ESA NO_2 in support of CO_2

Table 2: Total annual CO_2 emissions and NO_2 emissions over the Iberian Peninsula.

Emissions Tg/yr	TNO CO_2	TNO CO_2	DECSO CO_2	DECSO CO_2	DECSO CO_2
filter	-	*TNO NO_2 > 10^8 g/grid/yr*	-	*TNO NO_2 > 10^8 g/grid/yr*	*TNO NO_2 > 10^8 g/grid/yr TNO CO_2 > $5 \cdot 10^9$ g/grid/yr*
2010	341.8	290.7	581.7	390.6	372.2
2015	332.1	271.6	637.9	399.8	382.9
Emissions Tg/yr	**TNO NO_2**		**DECSO NO_2**	**DECSO NO_2**	
filter	-		-	*TNO NO_2 > 10^8 g/grid/yr*	
2010	1.49		2.55	1.41	
2015	1.36		2.55	1.37	

The uncertainty on the total numbers of CO_2 emissions given in this report depend on various aspects of the method as summarised in Table 2. When using TROPOMI observations, the uncertainty on the uncertainties will affect the NO_2 emissions. DECSO provides emissions together with the error estimates. And from these results we can estimate the uncertainty of 2-3 % on the total CO_2 emissions as a result of the uncertainty in DECSO [Ding et al., 2017a]. Note that this uncertainty only reflect random errors, not biases. The intercountry differences in the ratio (see Figure 8) as discussed before will add another 10% to the uncertainty. The difference in the year of the ratios (2015) and the NO_2 emissions (2018-2019) will also add to the uncertainty. The range given here represents the 95% interval. However, the probability distribution of the time differences in ratio is non-Gaussian. The 99% interval values are -10 to 43%, respectively. The error introduced by the background correction is more difficult to estimate. However, we estimated this as about 10% of additional uncertainty.

Table 3: Uncertainty analysis on total CO_2 for the Iberian peninsula

Cause of uncertainty	Estimated uncertainty	Possible future improvements
Uncertainty in NO_2 emissions	2-3 %	Further research on DECSO
Intercountry ratio differences	10 %	Uniform reporting methods
Time differences in ratio	-2 to 16 % per year	Apply the same year for the ratio and the NO_2 emissions
Correction biogenic NO_2 emissions	10 %	1) Other correction methods 2) Distinguish biogenic and anthropogenic emissions in DECSO

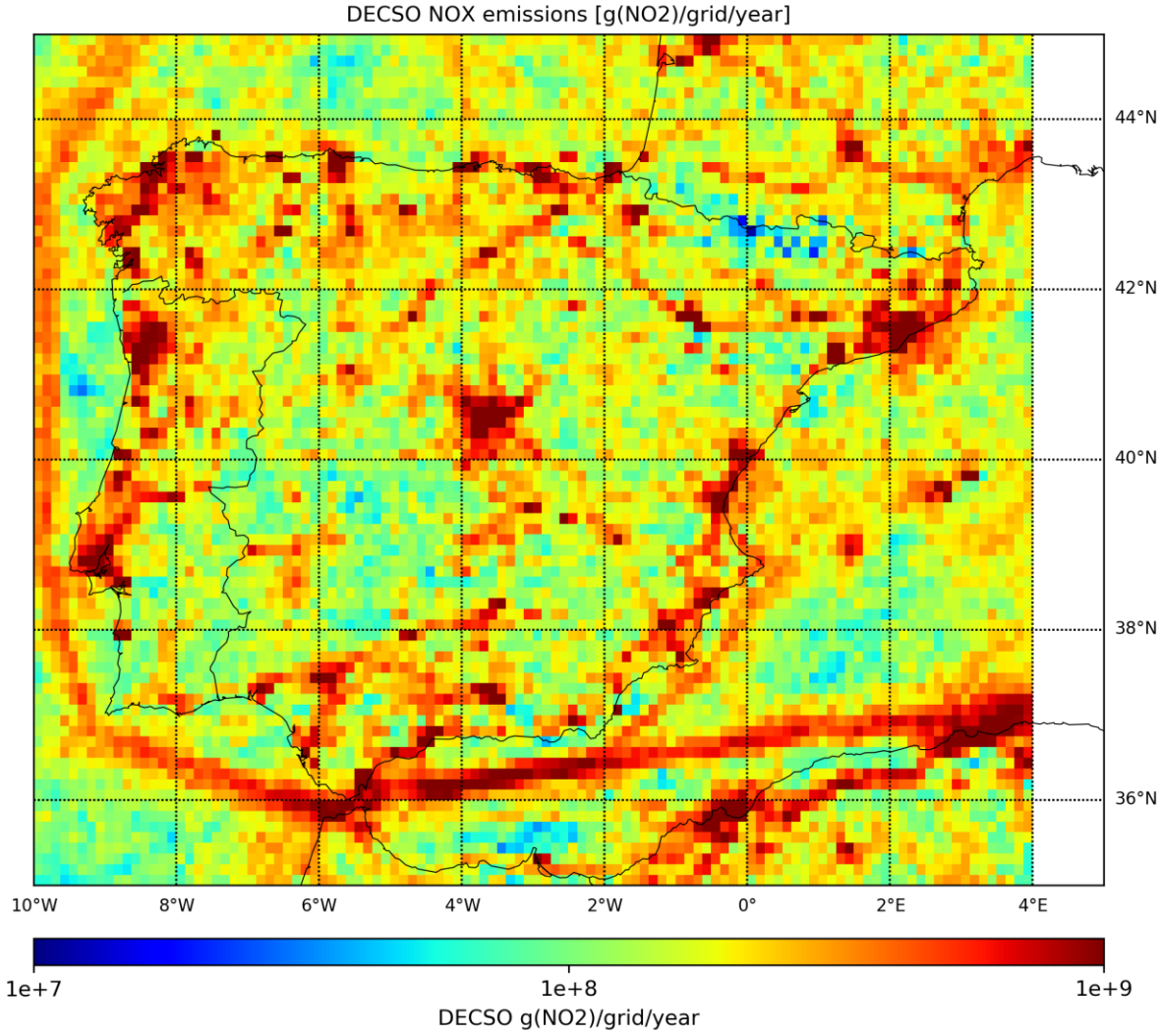

Figure 1a. DECSO NO_2 emissions [g(NO_2)/grid/year; 2018/2019] at a 0.125° spatial resolution for the Iberian peninsula based on TROPOMI tropospheric NO_2 measurements.

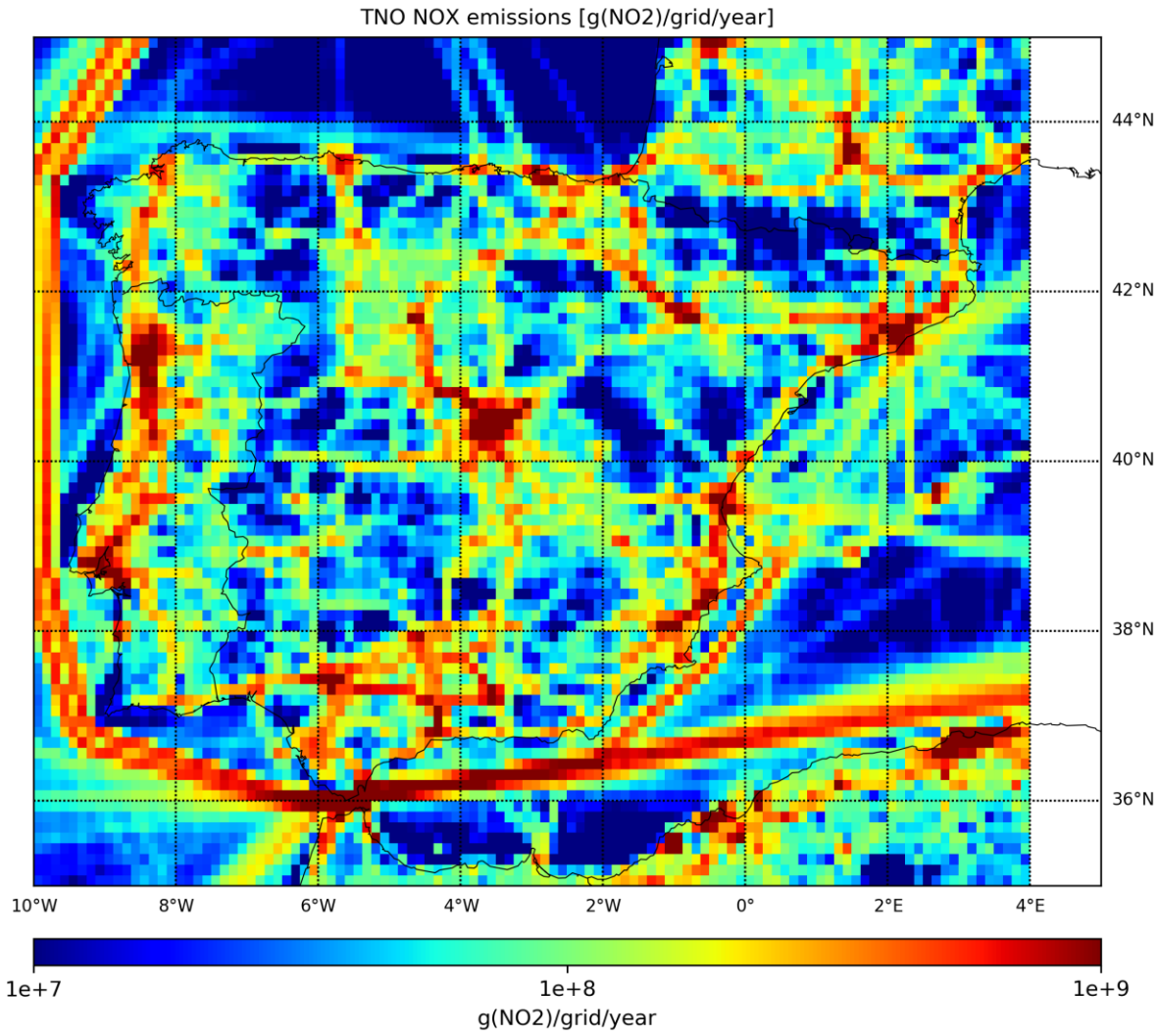

Figure 1b. TNO anthropogenic NO_2 emissions [g(NO_2)/grid/year] for 2015 for the Iberian peninsula. Data is regridded to a 0.125° spatial resolution from the original 0.1° spatial resolution. Courtesy H. Denier van der Gon, 2019.

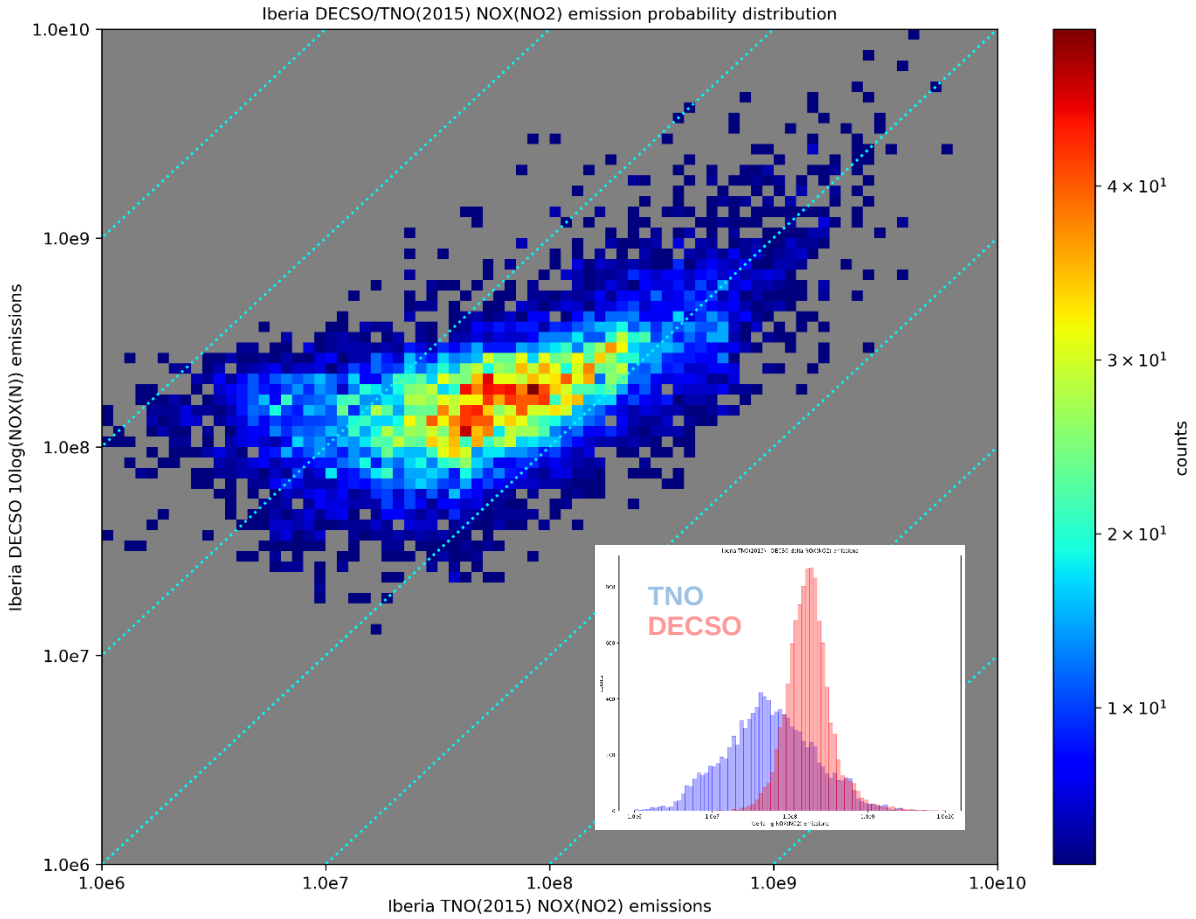

Figure 2. Probability distribution of DECSO NO_2 emissions (2018/2019) against TNO 2015 NO_2 emissions for the Iberian peninsula (figures 1a and 1b) on a log-log scale. Dotted lines are for reference only, spatial resolution of both datasets is 0.125°. The insert shows both probability distributions (pink: DECSO, blue, TNO).

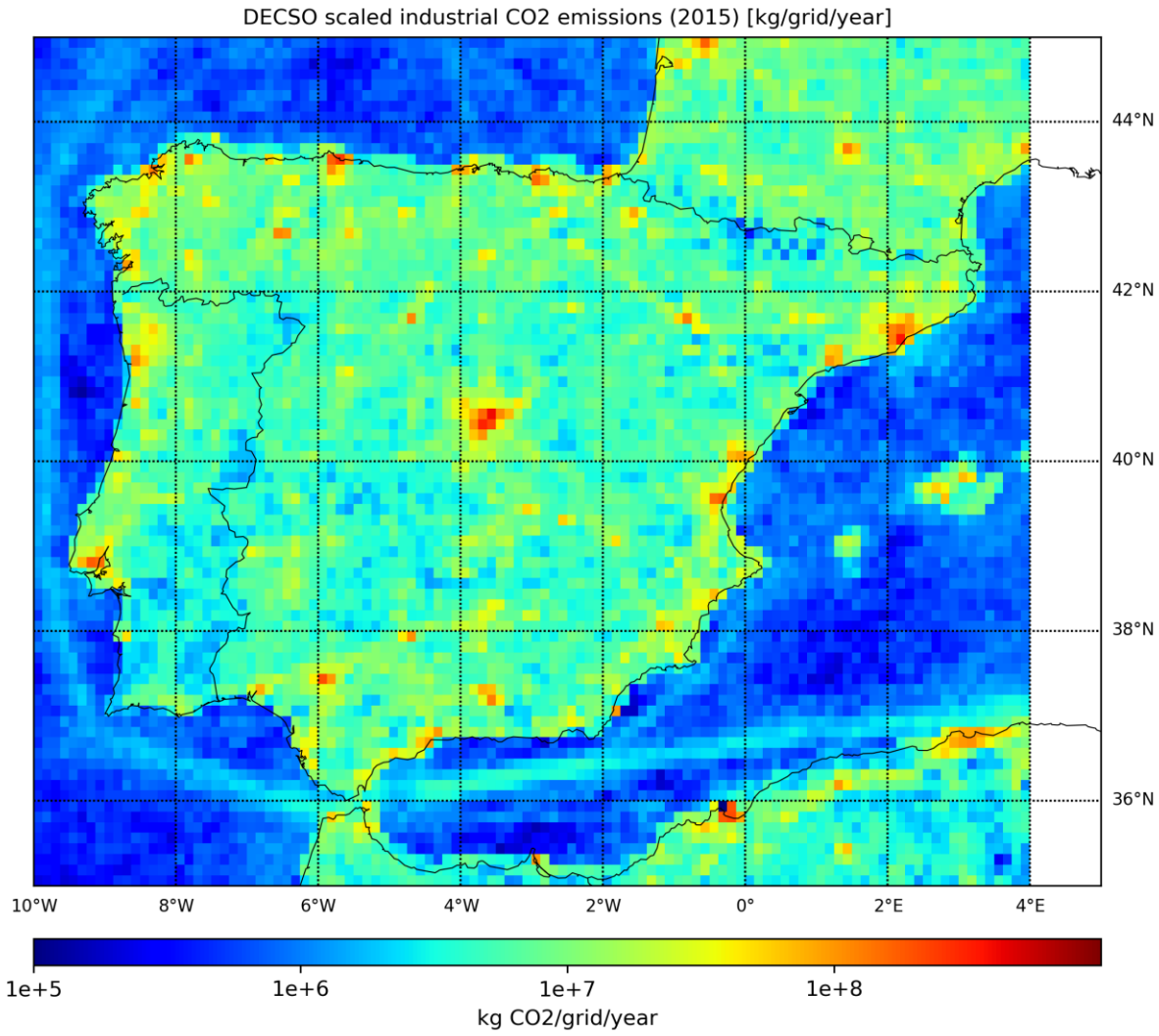

Figure 3a. CO_2 emissions [kg CO_2/grid/year] on a spatial resolution of 0.125° based on the multiplication of the DECSO-TROPOMI NO_2 emissions with the TNO 2015 CO_2/NO_2 emission ratio.

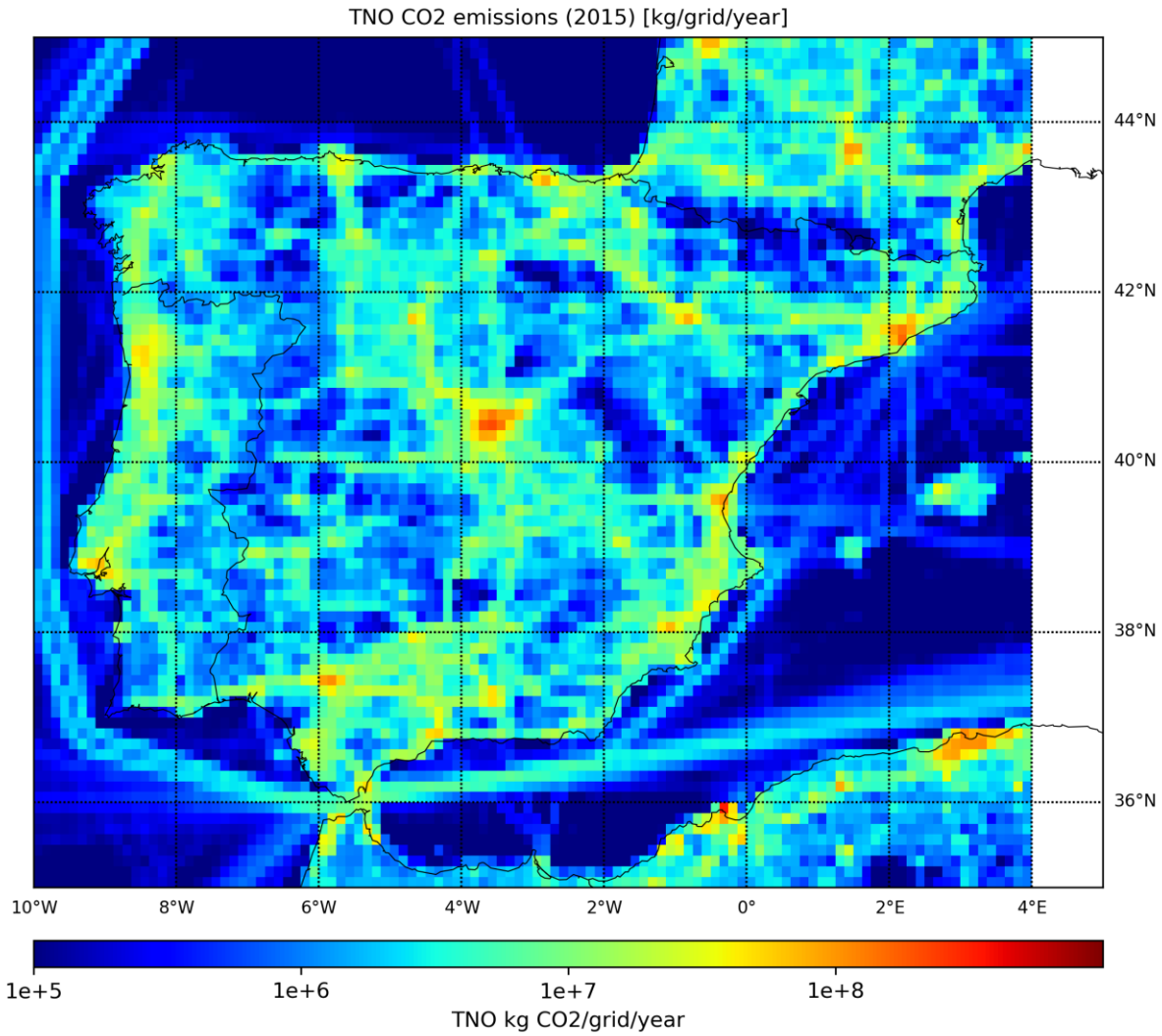

Figure 3b. TNO anthropogenic CO_2 emissions [kg CO_2/grid/year] on a spatial resolution of 0.125°.

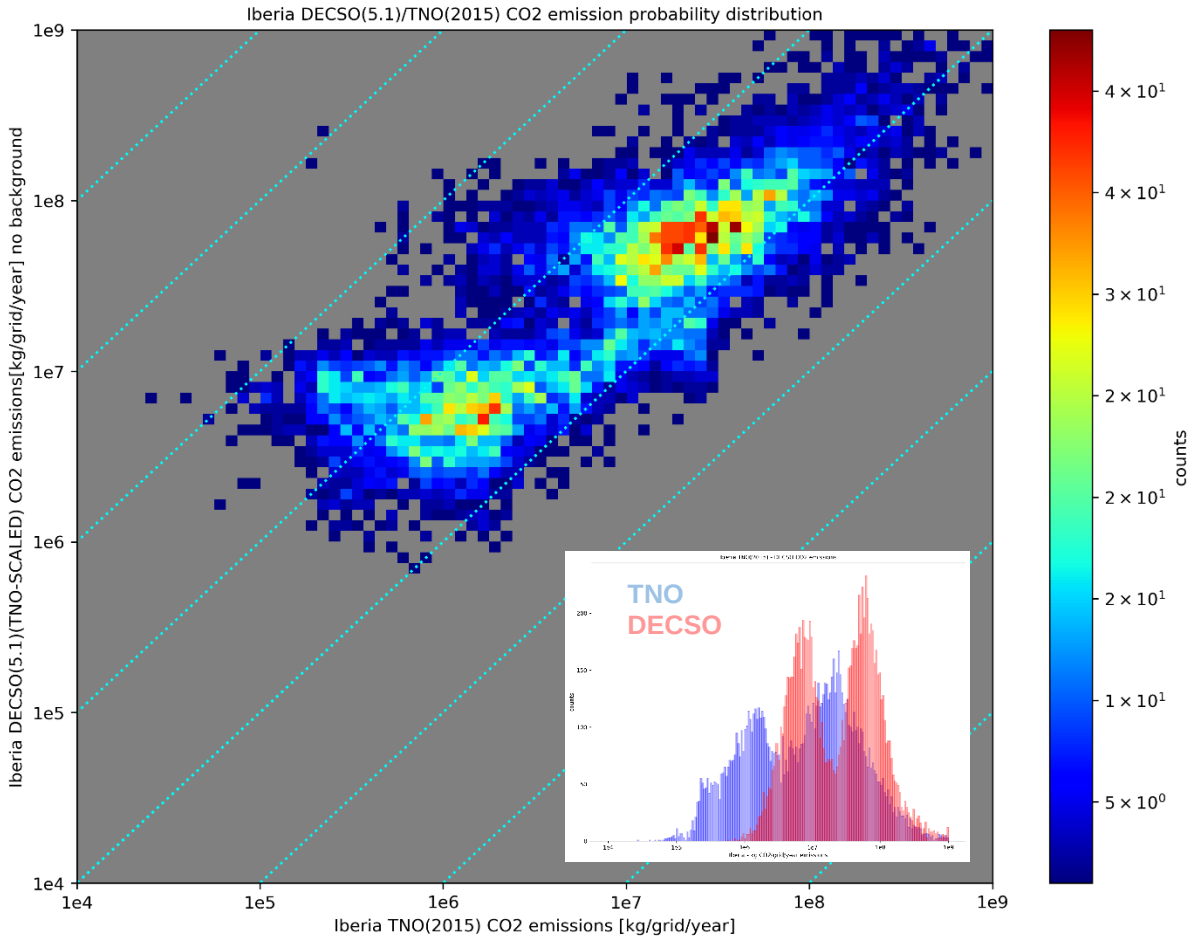

Figure 4. Probability distribution of DECSO-TROPOMI CO_2 emissions against TNO 2015 CO_2 emissions for the Iberian peninsula (figures 3a and 3b) on a log-log scale. Dotted lines are for reference only, spatial resolution of both datasets is 0.125°. The insert shows both probability distributions (pink: DECSO, blue, TNO).

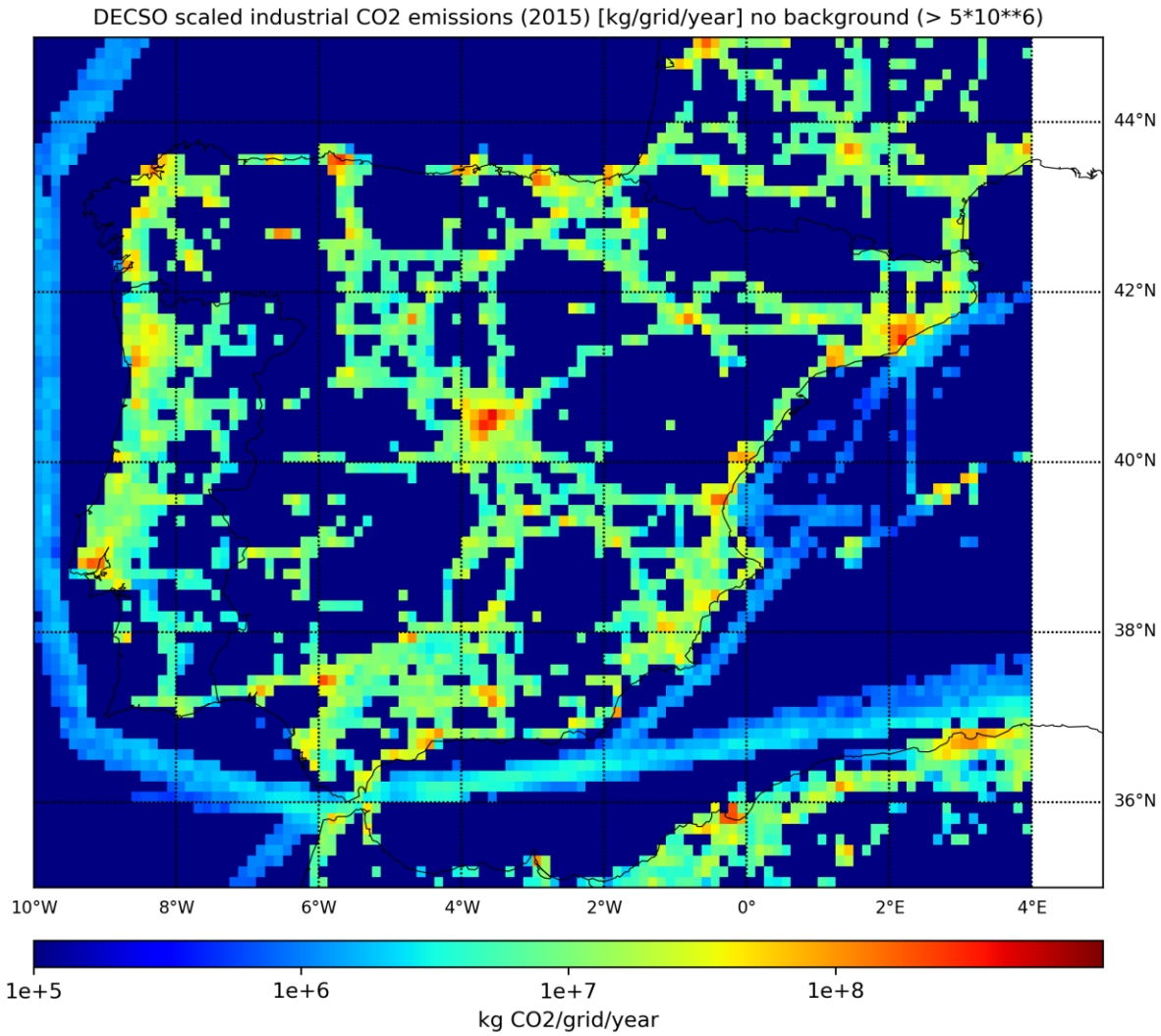

Figure 5a. As figure 3a but only showing TNO 2015 CO_2 emission > 5 10^6 kg/grid/year.

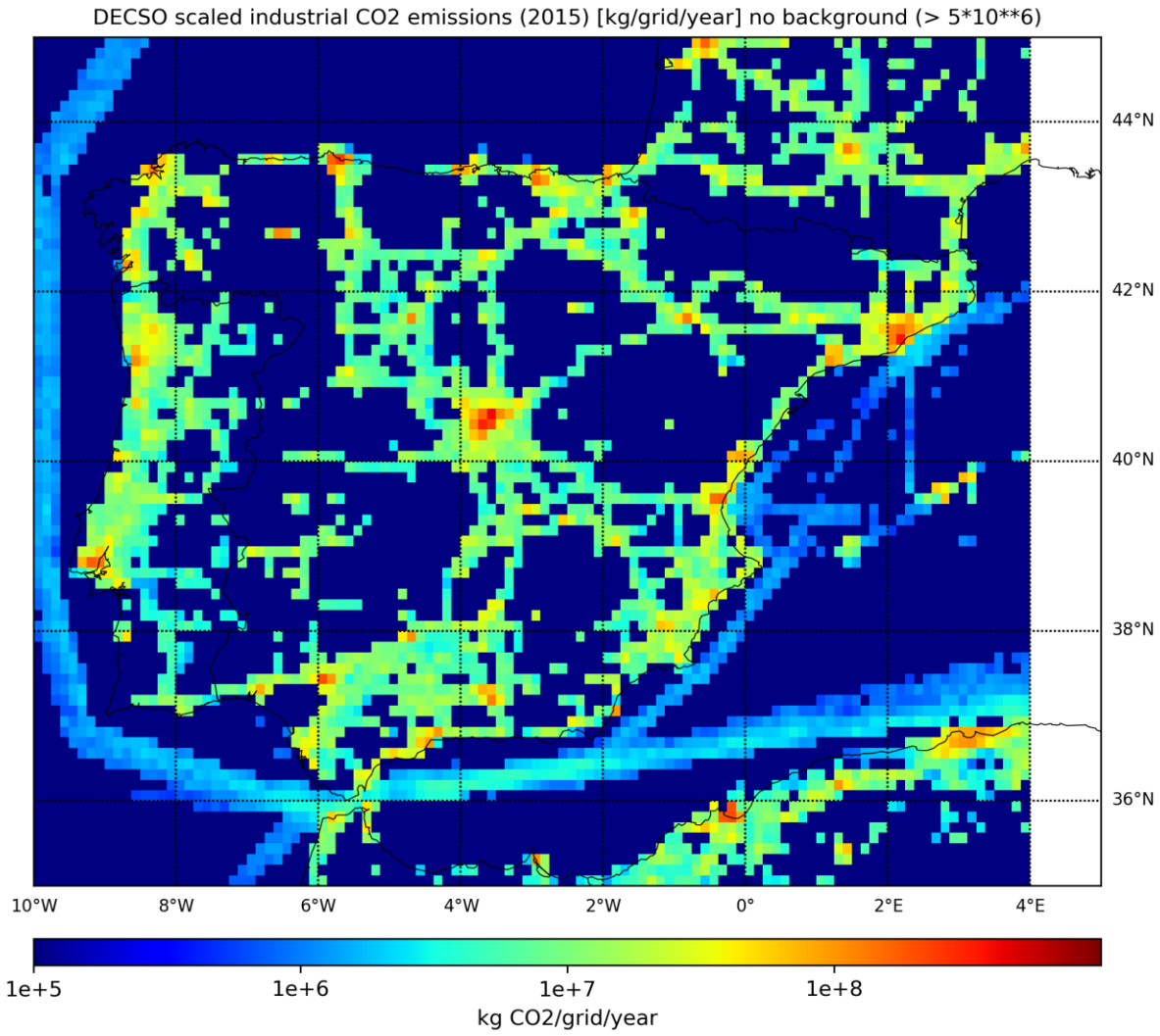

Figure 5b. DECSO-TROPOMI CO_2 emissions for CO_2 emissions > 5 10^6 kg/grid/year with 5 10^6 kg/grid/year subtracted. This background CO_2 level arises due to soil NO_2 emissions, which translate with the ratio method into non-physical CO_2 emissions.

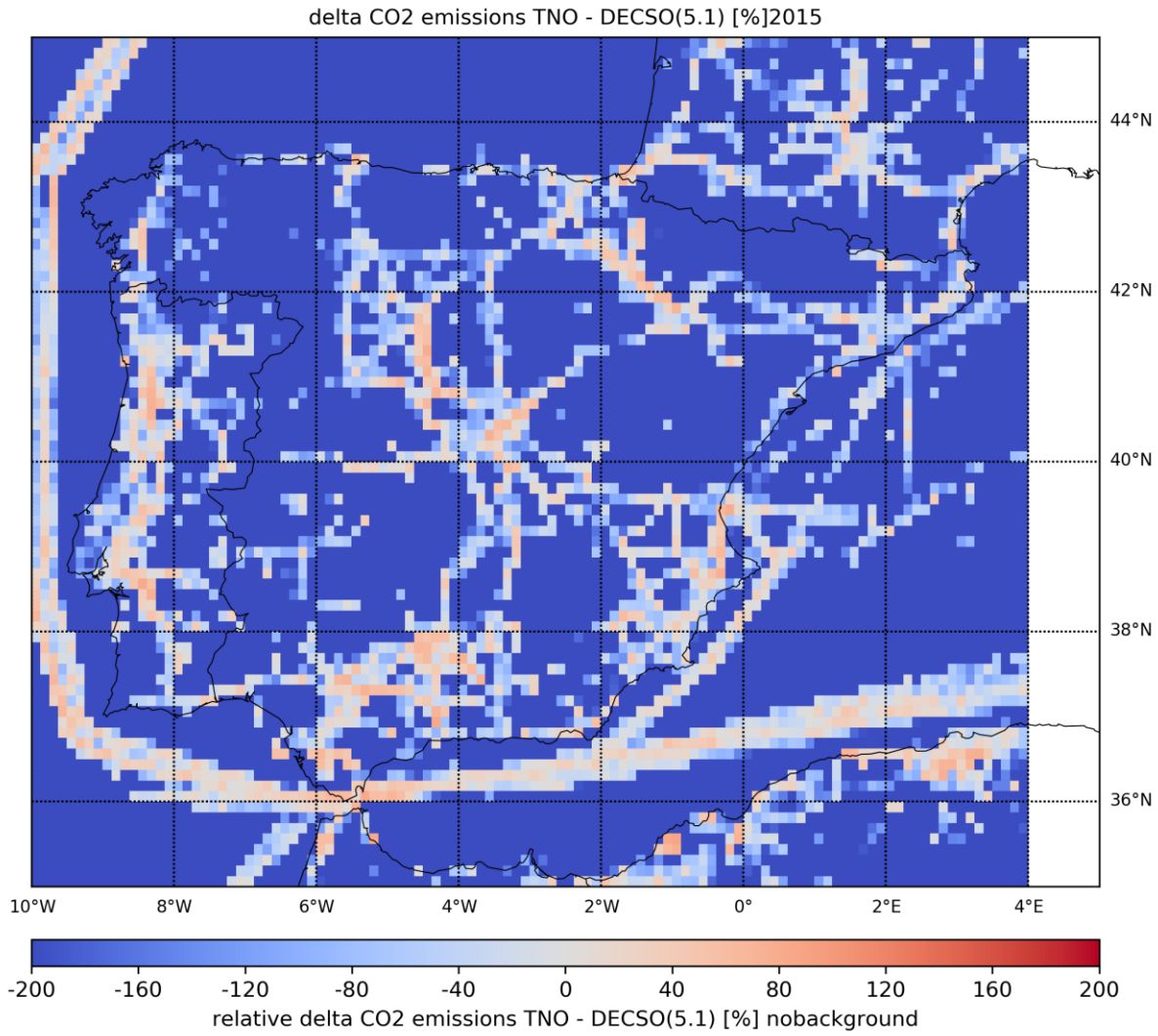

Figure 6a. Relative difference [%] in CO_2 emissions between TNO (Figure 5a) and DECSO-TROPOMI based CO_2 emissions corrected for soil NO_2 emission (see Figure 5b).

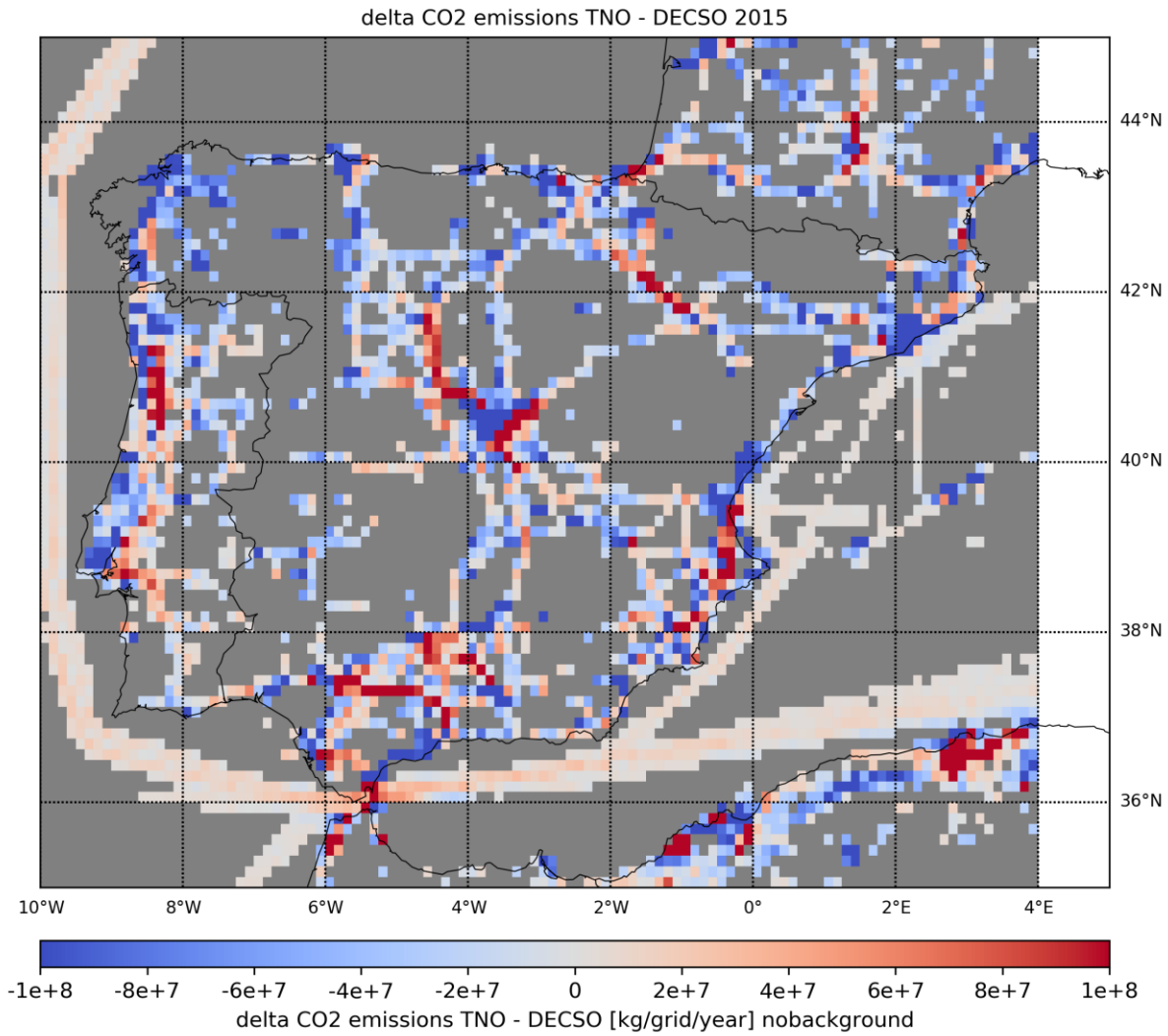

Figure 6b. As Figure 6a but for absolute CO_2 emissions differences.

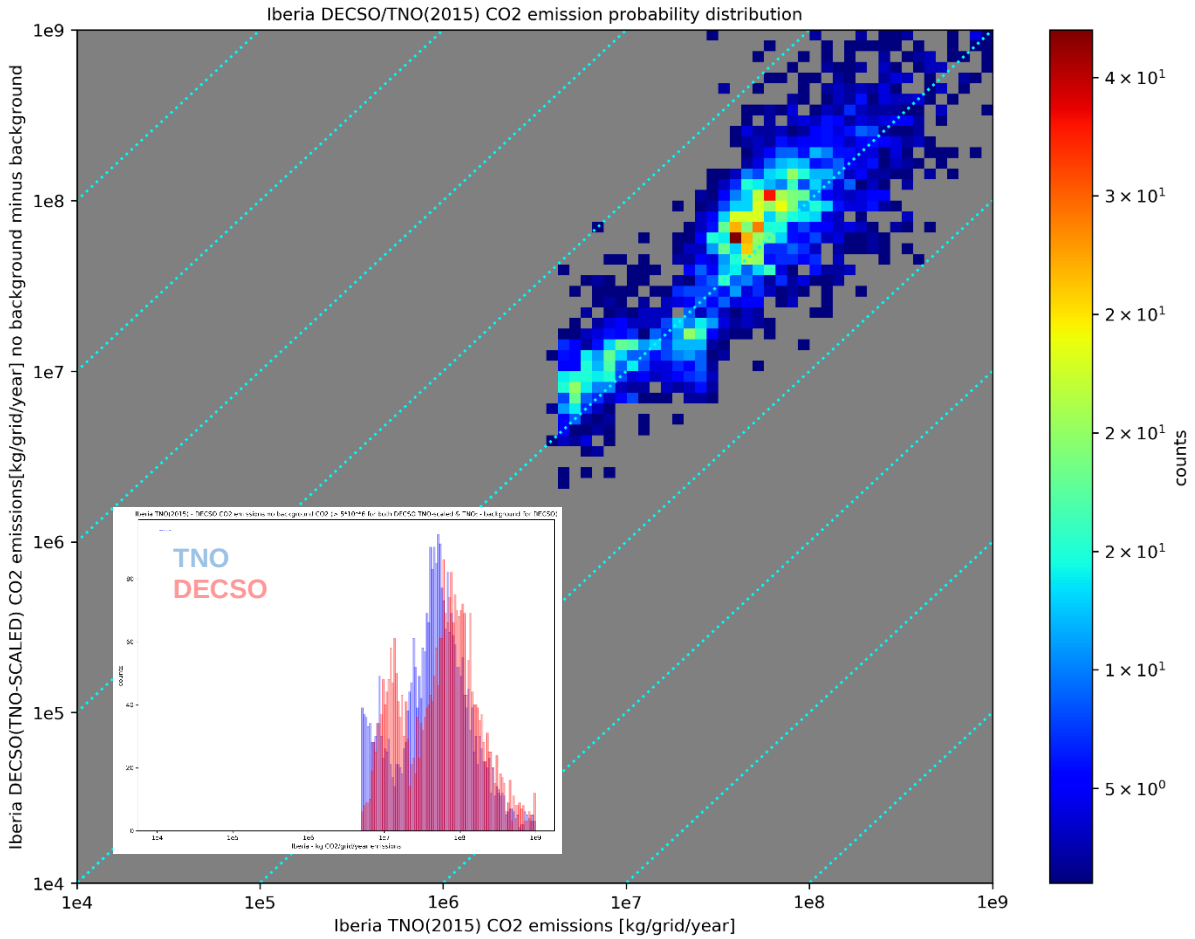

Figure 7. As Figure 5 but only for TNO 2015 CO_2 emissions > 5 10^6 kg CO_2/grid/year and TNO 2015 NO_2 emissions > 1 10^8 g NO_2/grid/year.

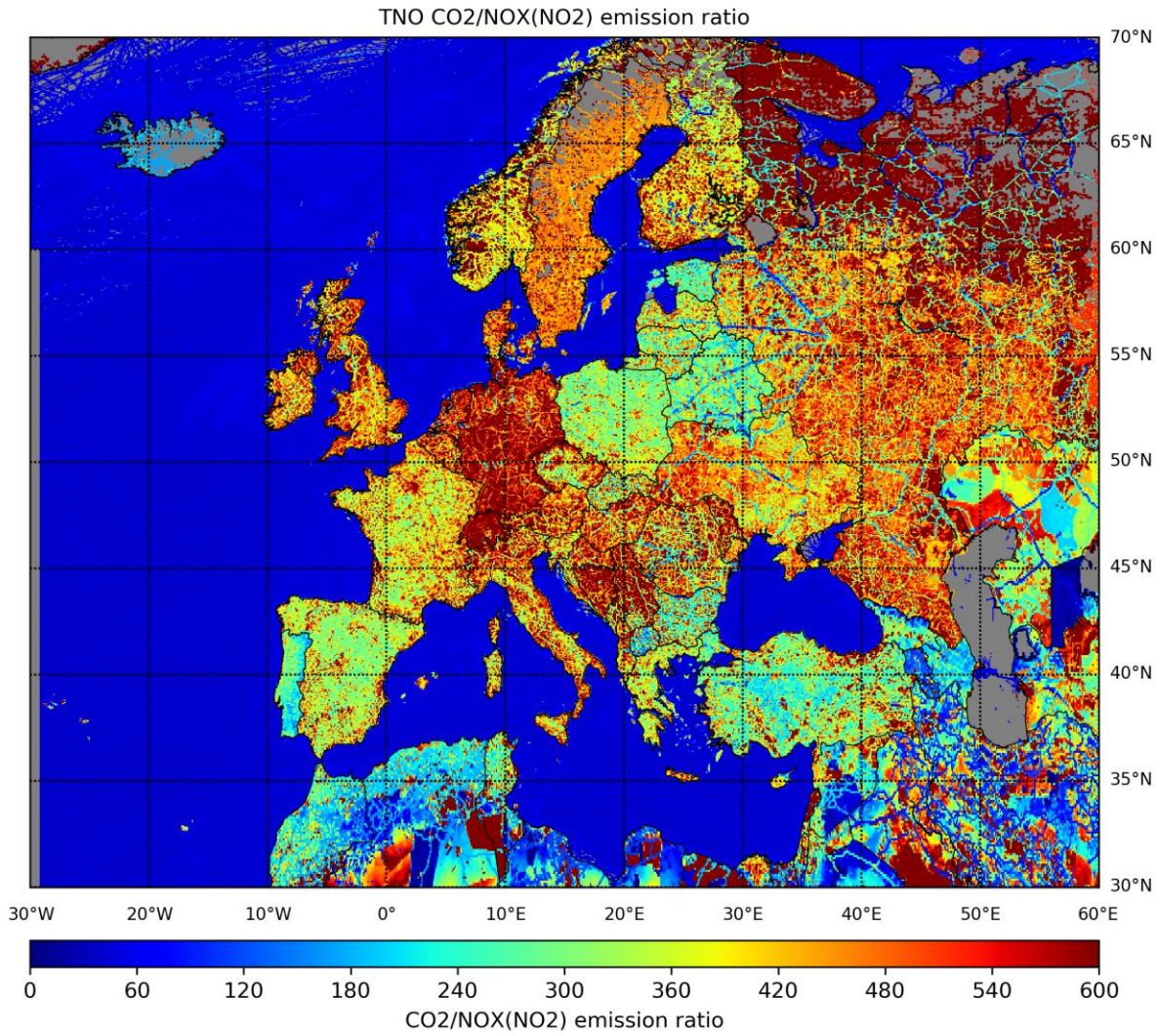

Figure 8. Ratio of TNO 2015 anthropogenic CO_2 emissions over TNO 2015 anthropogenic NO_2 emissions for the European domain on a 0.125° resolution.

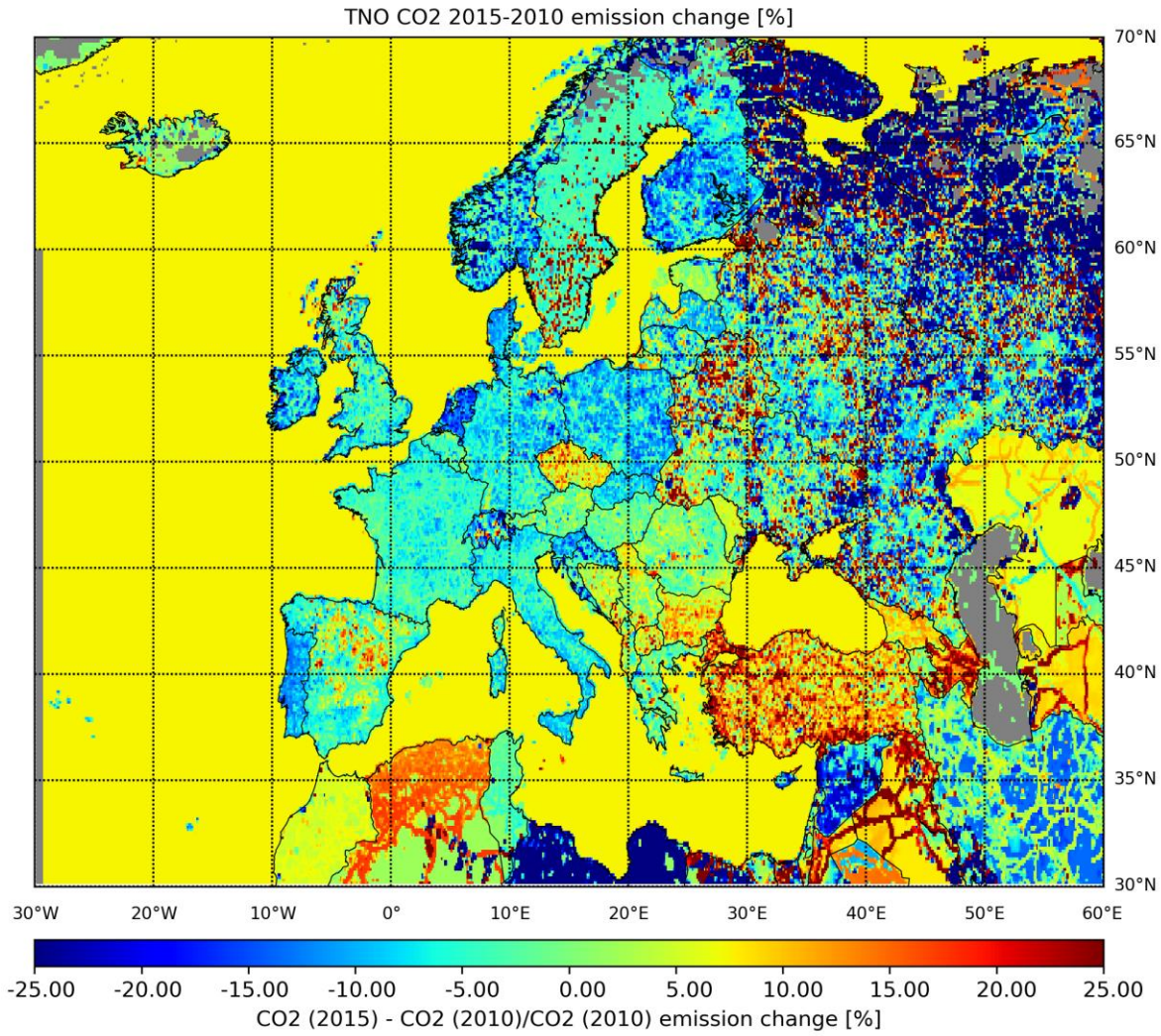

Figure 9a. Relative difference in TNO CO_2 emissions between 2010 and 2015.

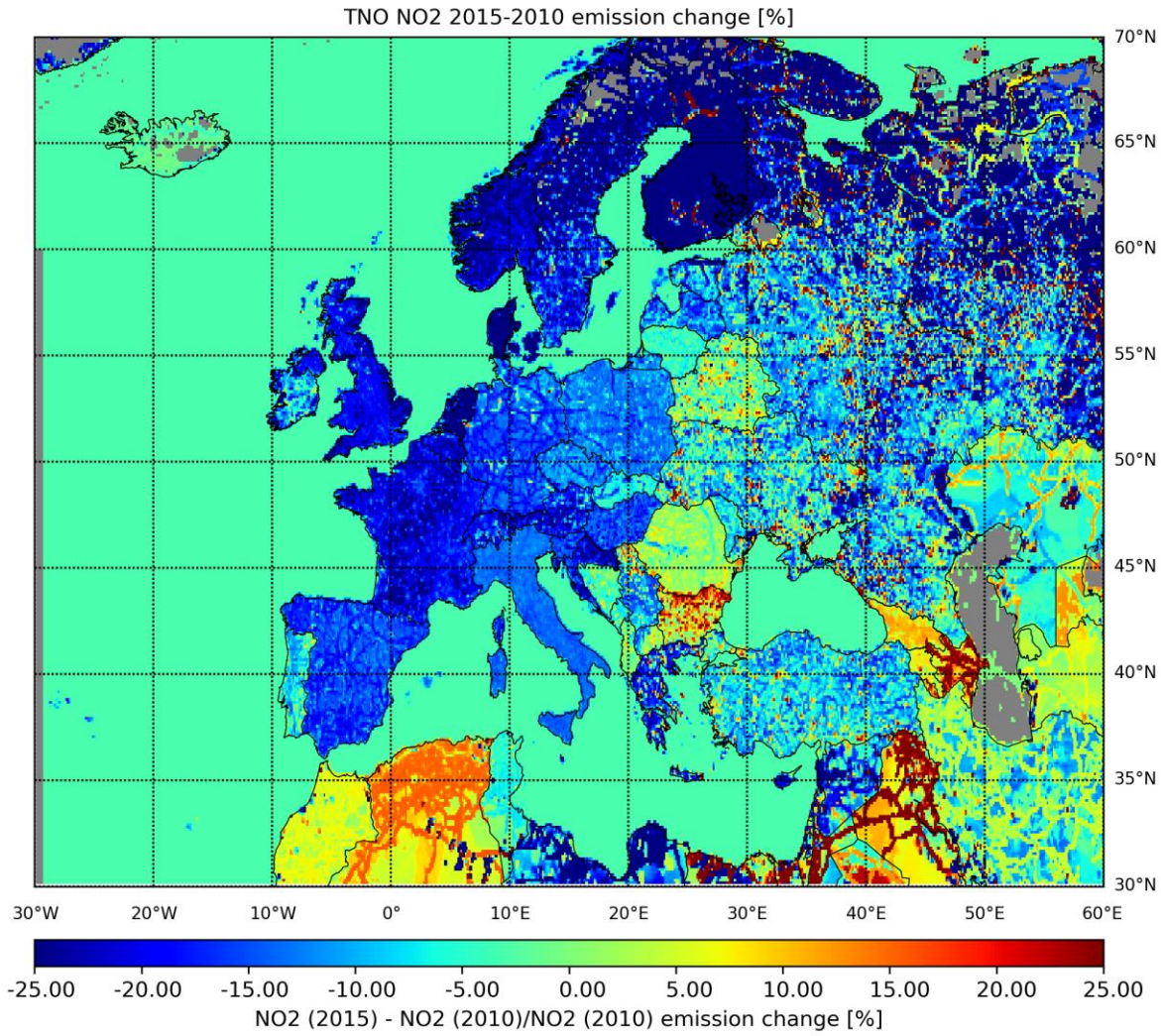

Figure 9b. As Figure 8 but for TNO anthropogenic NO_2 emissions.

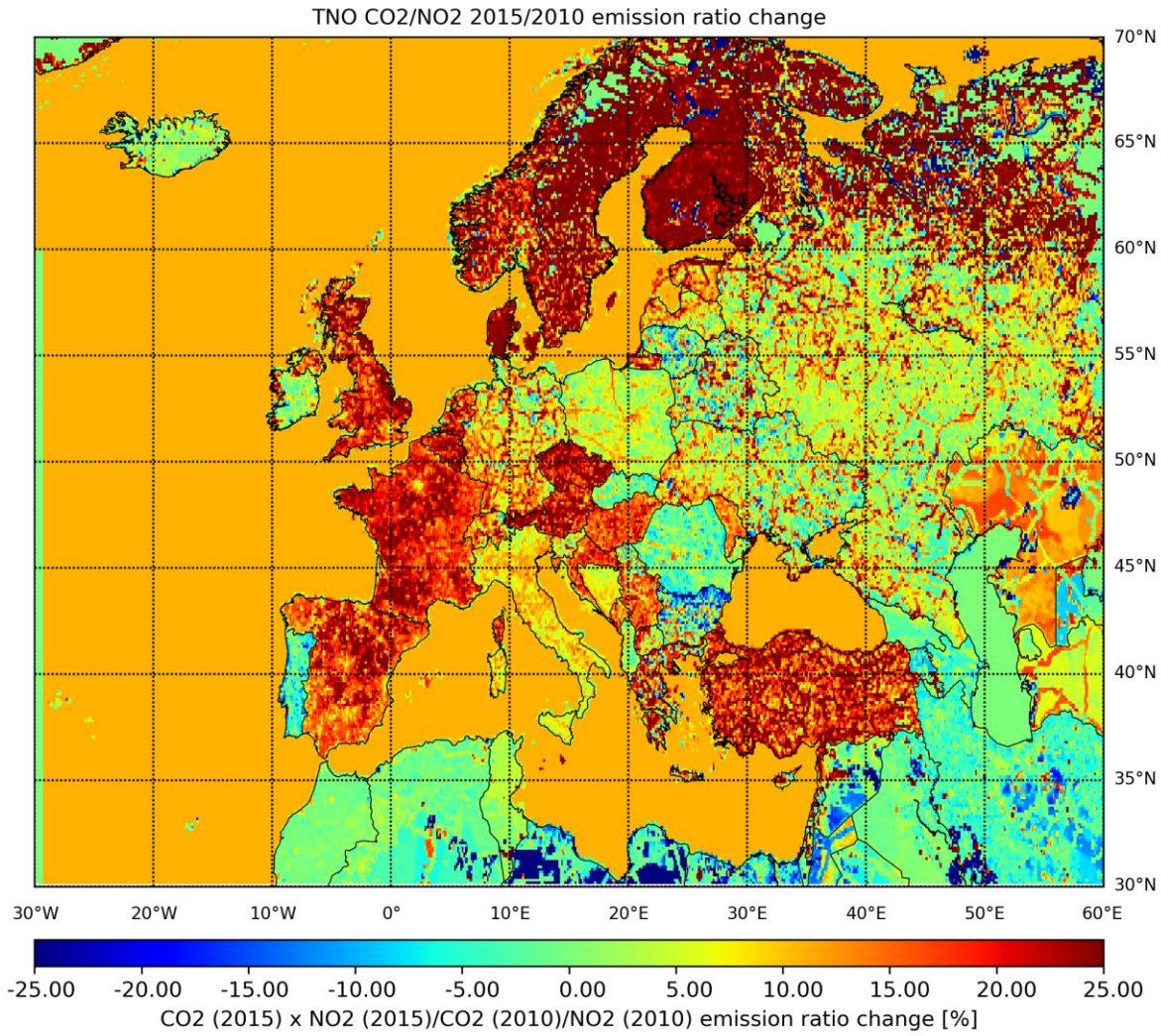

Figure 9c. As Figure 8 but for TNO anthropogenic CO_2 over NO_2 ratios.

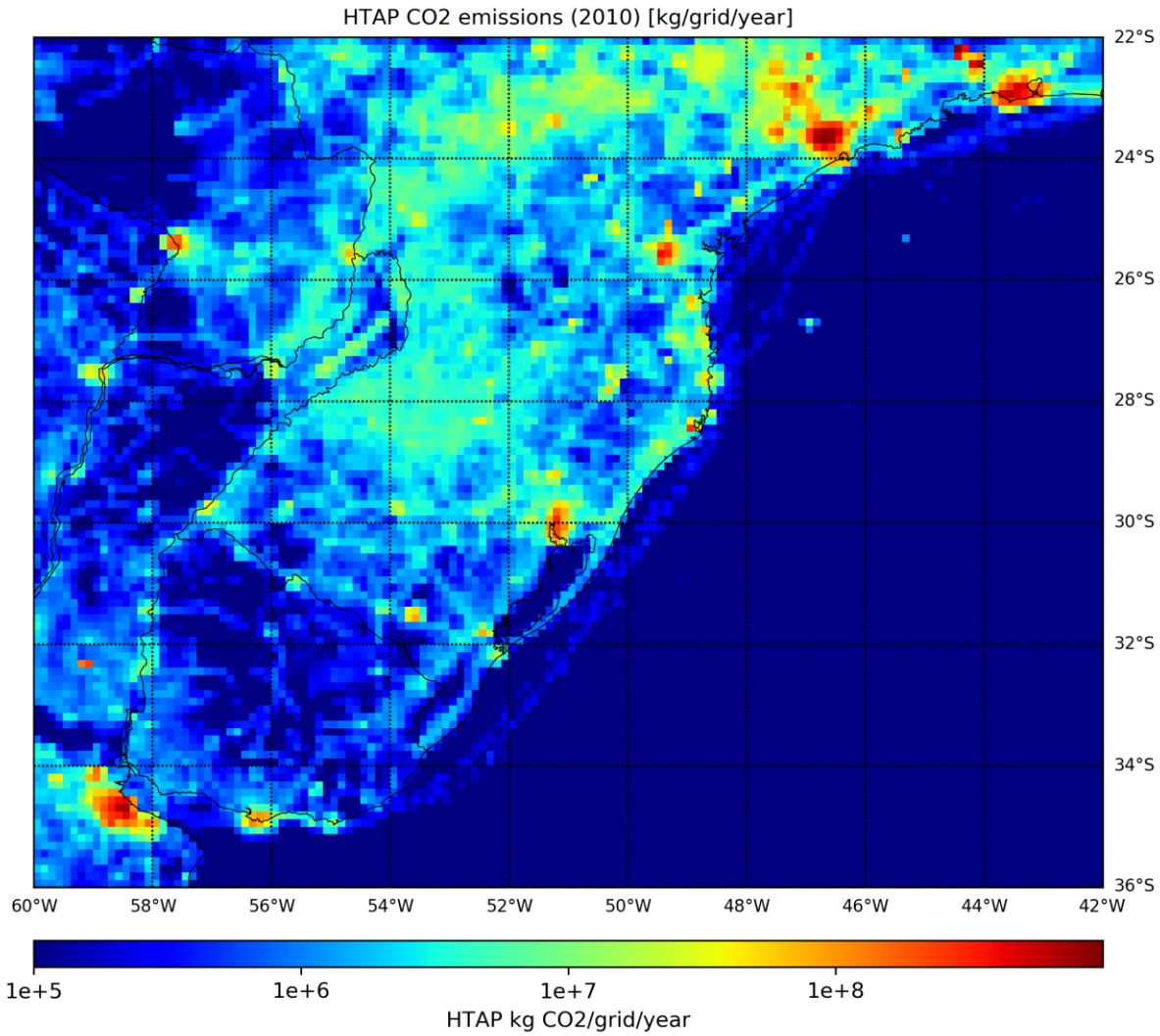

Figure 10a. EDGAR-HTAP v2 anthropogenic CO_2 emissions [kg CO_2/grid/year] on a spatial resolution of 0.125°.

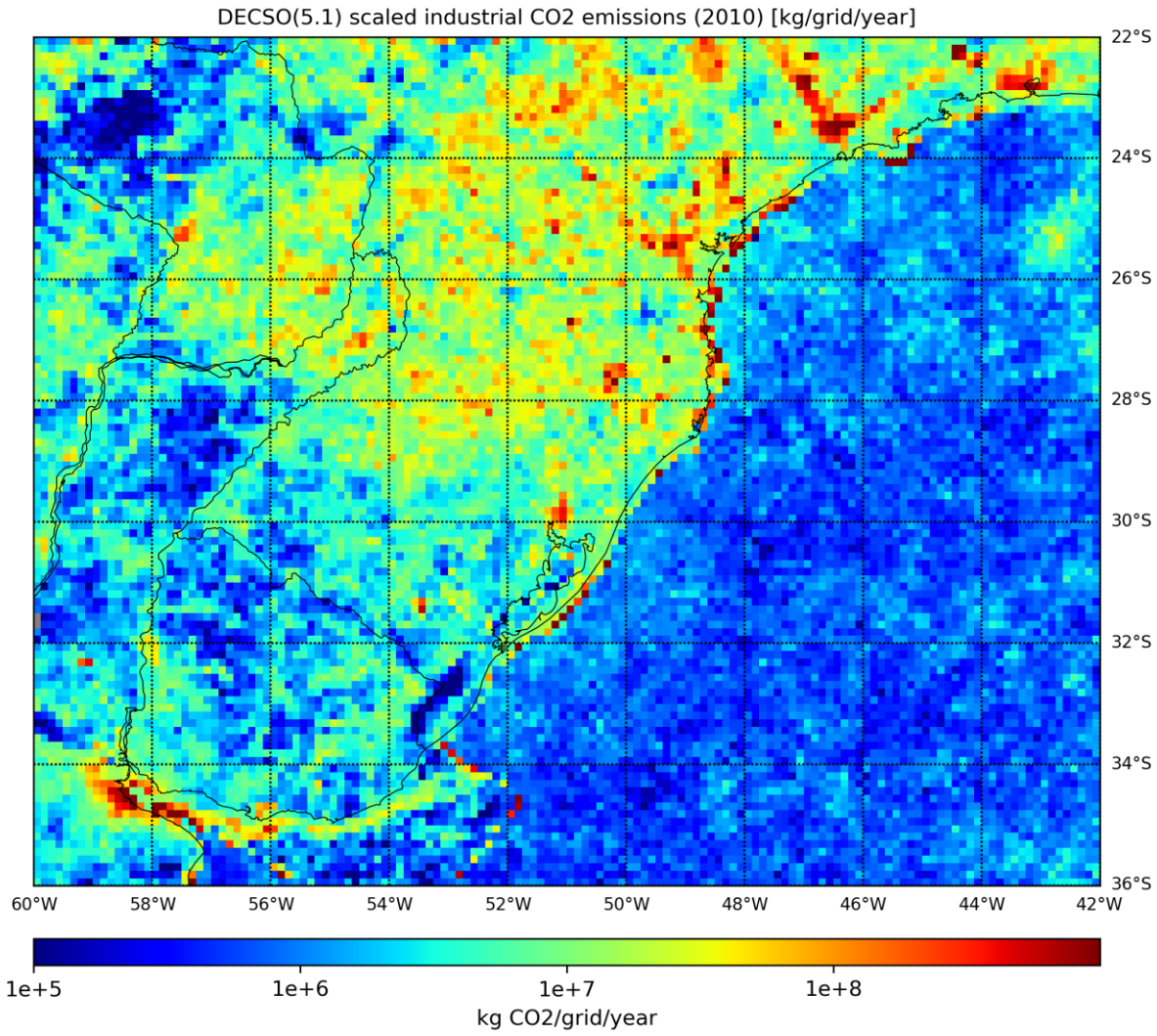

Figure 10b. CO_2 emissions [kg CO_2/grid/year] on a spatial resolution of 0.125° based on the multiplication of the DECSO-TROPOMI NO_2 emissions with the EDGAR-HTAP v2 2010 CO_2/NO_2 emission ratio.

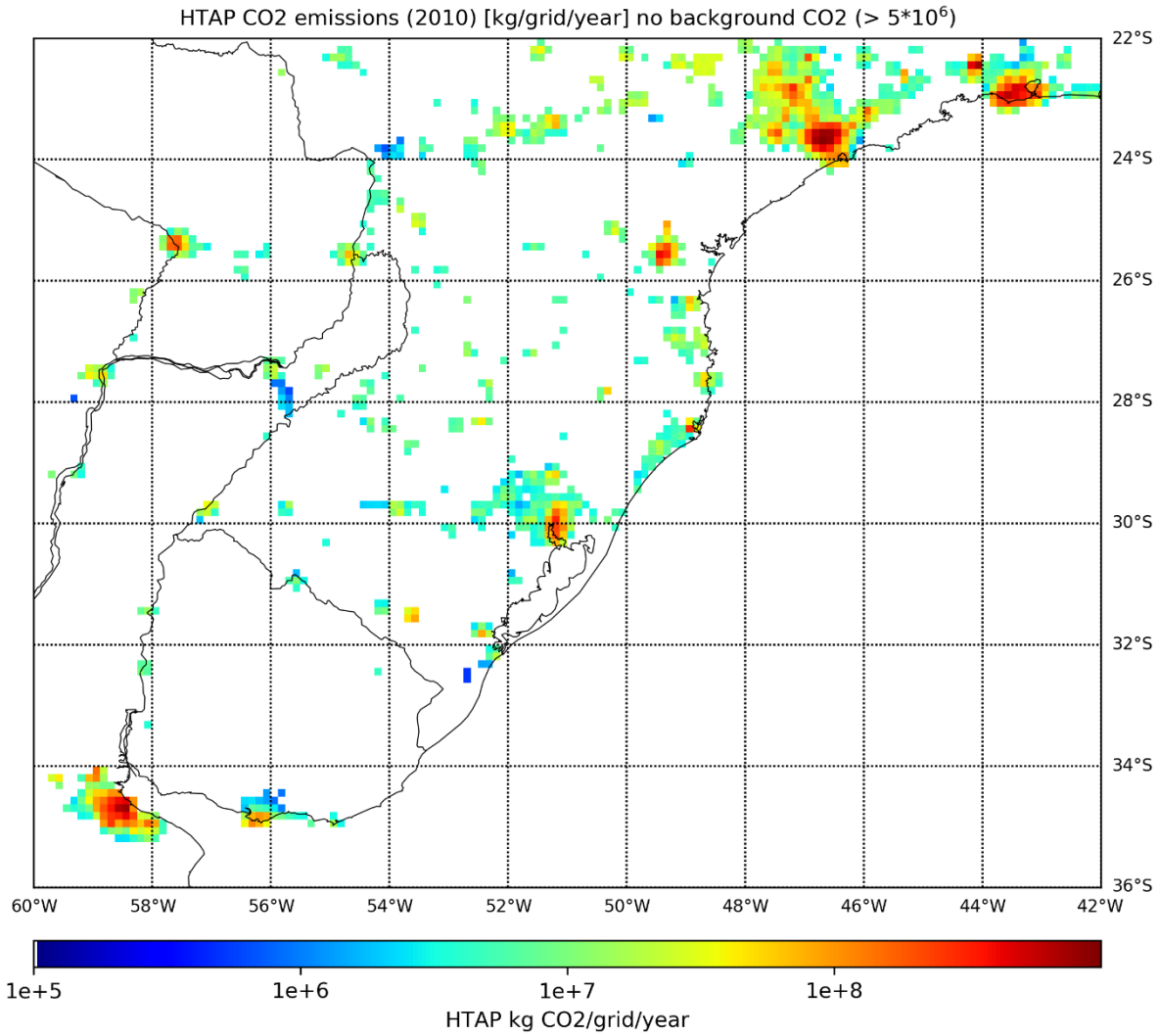

Figure 11a. As figure 10a but only grids with DECSO CO_2 emissions > 5 × 10^6 g/grid/year.

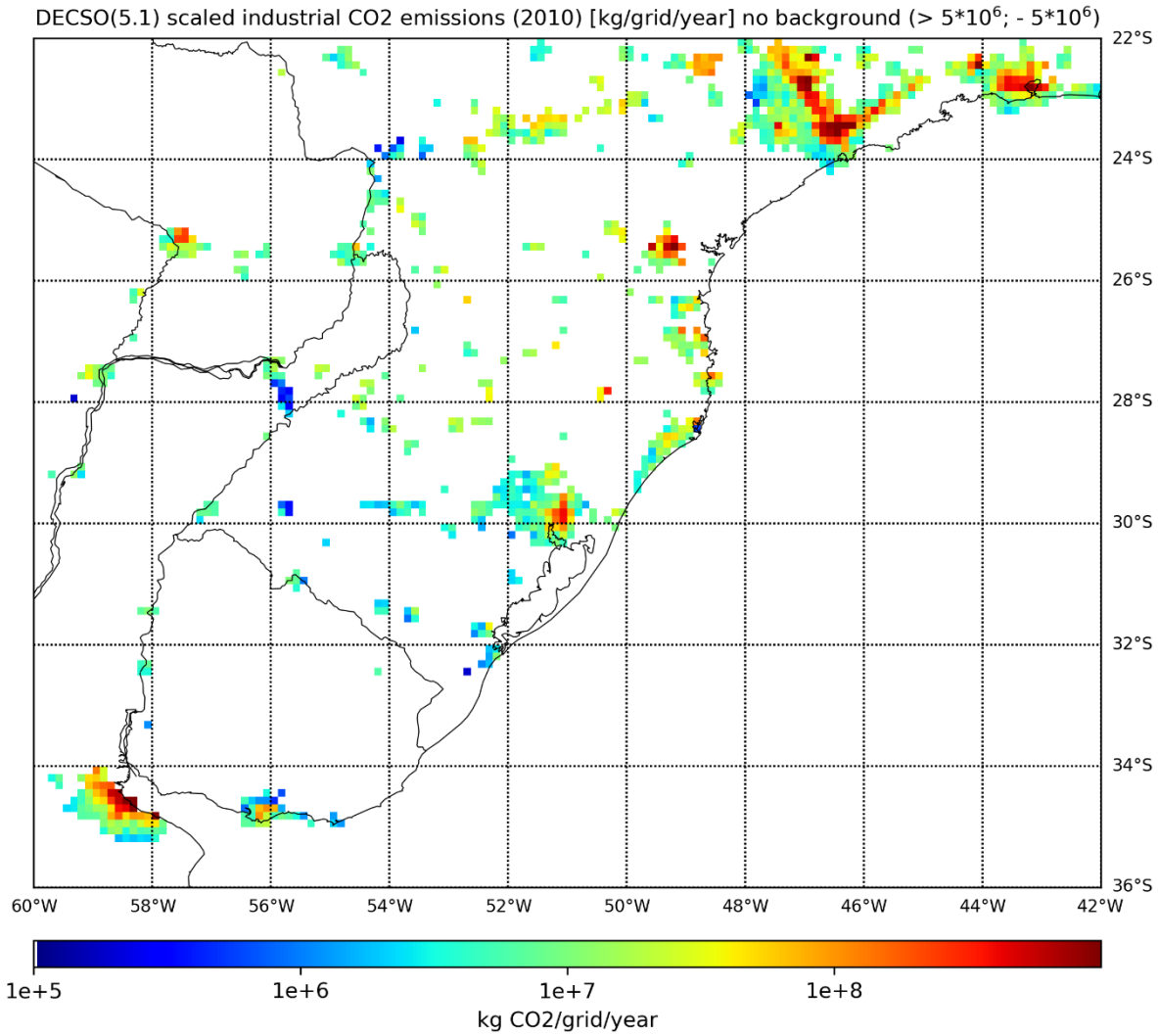

Figure 11b. As figure 10b but only showing grids with DECSO CO_2 emissions > 5 × 10^6 kg/grid/year, and subtracting a background CO_2 emission level of 5 × 10^6.

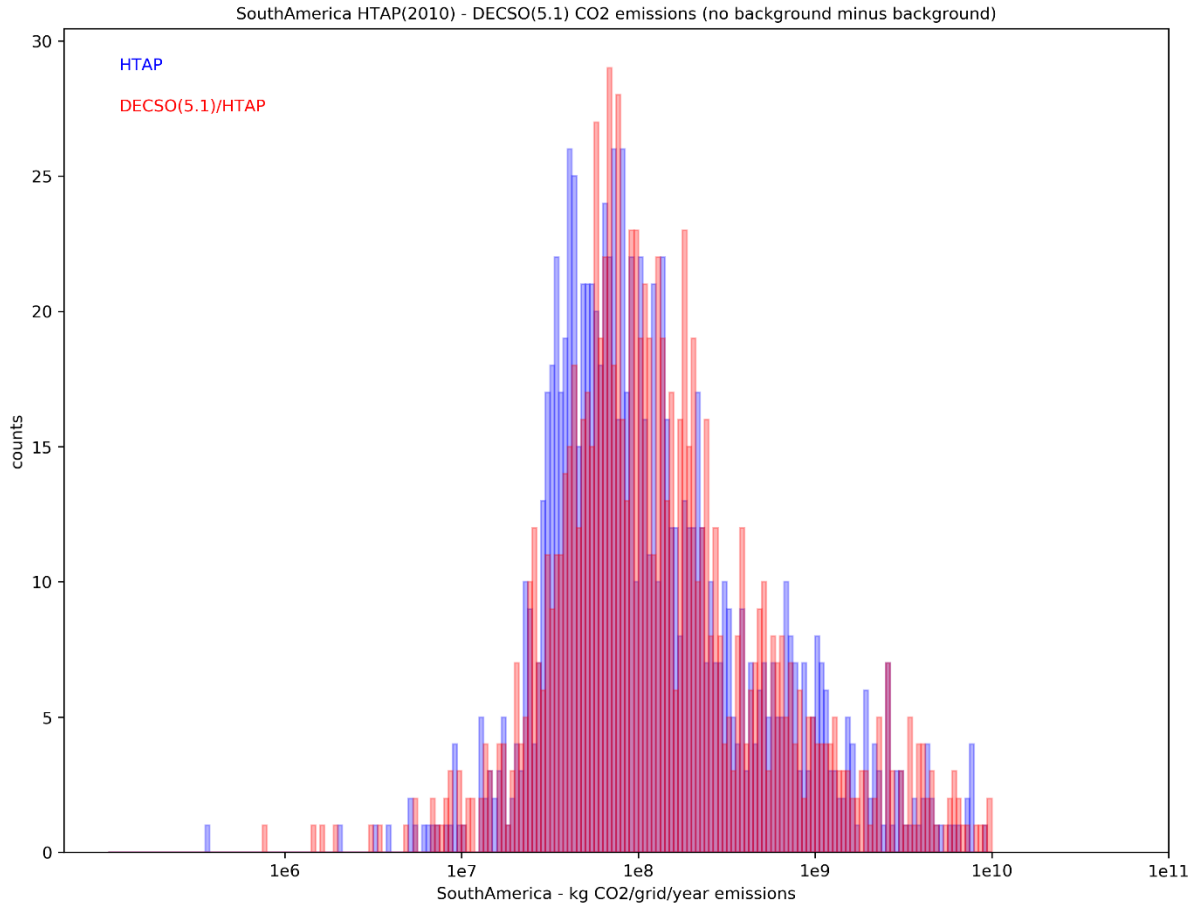

Figure 12. histogram of EDGAR-HTAP v2 and DECSO-TROPOMI based CO_2 emissions in kg CO_2/grid/year over the area in South America as shown in Figures 10 and 11. Only showing grids with DECSO CO_2 emissions > 5×10^6 kg/grid/year, while subtracting a background CO_2 emission level of 5×10^6 from DECSO CO_2 emissions.

7 Conclusion

We have analyzed DECSO-TROPOMI NO_2 emissions for the Iberian Peninsula and an area over South America and derived CO_2 emissions based on multiplying the DECSO-TROPOMI NO_2 emissions with CO_2 over NO_2 emission ratios derived from a TNO emissions database.

DECSO-TROPOMI NO_2 and associated CO_2 emissions have been compared with the TNO emissions themselves as a “sanity check”. The comparison has revealed the following

- The spatial distributions of NO_2 emissions over the Iberian Peninsula appear similar (also for South America, which was not shown here)
- The NO_2 soil emissions need to be accounted for as they translate into non-existing CO_2 emissions if the emission ratio method is applied
- One example of how to account for biogenic NO_2 emissions was provided here
- The spatial distribution of DECSO-TROPOMI based CO_2 emissions of the Iberian Peninsula and the South America region overall appears realistic, especially if NO_2 soil emissions are accounted for.
- The spatial patterns of TNO emissions ratios reveal strong inter-country differences

- The spatial patterns over the Iberian Peninsula of TNO emission changes between 2010 and 2015, as well as the ratio of emission ratios, confirm the existence of strong inter-country differences

Based on these findings we identify the following topics that are in need of further attention:

- For a proper application of this method, satellite observations of NO_2 of the year for which the ratios are valid should be used.
- Additional effort is needed to further investigate methods on how to account for biogenic NO_2 emissions
- The presence of inter-country differences in CO_2 over NO_2 emission ratios suggest the presence of country-specific emission registration methods and/or emission calculation methods.

8 References

Ding, J., Miyazaki, K., van der A, R.J., Mijling, B., Kurokawa, J., Cho, S., Janssens-Maenhout, G., Zhang, Q., Liu, F., and Levelt, P.F. (2017a), Intercomparison of NOx emission inventories over East Asia, Atm. Chem. Phys., 17, 10125-10141, doi:doi.org/10.5194/acp-17-10125-2017.

Ding, J., R.J. van der A, B. Mijling and P.F. Levelt (2017b), Space-based NOx emission estimates over remote regions improved in DECSO Atmospheric Measurement Techniques, 10, 925-938, doi:10.5194/amt-10-925-2017.

Ding, J., van der A, R. J., Mijling, B., Jalkanen, J.-P., Johansson, L. and Levelt, P. F. (2018), Maritime NOx emissions over Chinese seas derived from satellite observations. Geophysical Research Letters, 45. https://doi.org/10.1002/2017GL076788.

Janssens-Maenhout, G., Crippa, M., Guizzardi, D., Dentener, F., Muntean, M., Pouliot, G., Keating, T., Zhang, Q., Kurokawa, J., Wankmüller, R., Denier van der Gon, H., Kuenen, J. J. P., Klimont, Z., Frost, G., Darras, S., Koffi, B., and Li, M. (2012), HTAP_v2.2: a mosaic of regional and global emission grid maps for 2008 and 2010 to study hemispheric transport of air pollution, Atmos. Chem. Phys., 15, 11411–11432, https://doi.org/10.5194/acp-15-11411-2015.

Mijling, B., & van der A, R. J. (2012). Using daily satellite observations to estimate emissions of short-lived air pollutants on a mesoscopic scale. Journal of Geophysical Research: Atmospheres, 117(D17).

Veefkind, J. P.; Aben, I.; McMullan, K.; Förster, H.; de Vries, J.; Otter, G.; Claas, J.; Eskes, H. J.; de Haan, J. F.; Kleipool, Q.; van Weele, M.; Hasekamp, O.; Hoogeveen, R.; Landgraf, J.; Snel, R.; Tol, P.; Ingmann, P.; Voors, R.; Kruizinga, B.; Vink, R.; Visser, H.; and Levelt, P. F. (2012), TROPOMI on the ESA Sentinel-5 Precursor: A GMES mission for global observations of the atmospheric composition for climate, air quality and ozone layer applications, rse, 120: 70–83.

Document History

Version	Author(s)	Date	Changes
0.1	Jos de Laat (KNMI)	26/11/2019	First draft
0.2	Ronald van der A (KNMI)	5/12/2019	Editing and some new sections added
1.0	Jos de Laat	20/12/2019	Second draft considering review comments

Internal Review History

Internal Reviewers	Date	Comments
Tonatiuh Nuñez Ramirez (MPI-BGC, Jena)	06/12/2019	Approved with comments
(SPASCIA)	17/12/2019	Approved with comments

Estimated Effort Contribution per Partner

Partner	Effort
KNMI	2 person months
Total	2 person months